Physical Gelation of a Multiblock Copolymer: Effect of Copolymer Composition

Xiongwei He, Jean Herz, and Jean-Michel Guenet*

Institut Charles Sadron (CRM-EAHP), CNRS—Université Louis Pasteur, 6, rue Boussingault, 67083 Strasbourg Cedex, France. *Received September 30, 1987; Revised Manuscript Received December 4, 1987*

ABSTRACT: Investigations on the physical gelation of an organosilicic multiblock copolymer in *trans*-decalin are reported [poly(dimethylsiloxane)–poly[1-(dimethylsilyl)-4-(dimethylvinylsilyl)benzene]]. Particular attention is focused on the effects arising from the variation of the crystalline sequence content X_{COSP} (X_{COSP} = 10%, 20%, 50%). The temperature–concentration phase diagrams are established. They show through the occurrence of a monotectic transition that, in all cases, the gelation mechanism involves a liquid–liquid phase separation frozen in at its early stage by crystallization. The variations of the compression modulus E as a function of temperature and polymer concentration C are determined. At room temperature, it is found that E varies as $E \sim X_{COSP}^{2}C^{4.5\pm0.1}$. A tentative explanation is provided for these exponents. The swelling behavior in an excess of solvent is examined. A structural model made up with fiberlike entities is proposed to account for the results. The consequences of these findings on gels of atactic PVC are briefly discussed.

Introduction

Much effort is currently devoted to the study of polymer physical gelation. One endeavors to comprehend several aspects such as the molecular structure,[1-5] the thermodynamics of formation and fusion,[6-8] the mechanical properties,[9,10] and the like.

Interestingly, the propensity to form physical gels is not restricted to crystalline polymers. Some polymers, designated as atactic and accordingly regarded as uncrystallizable, display quite marked gelation properties under appropriate conditions. Among these, worth quoting are atactic polystyrene[6] and, more recently reported, poly(butyl methacrylate).[11] It is generally thought that the ordering of the highly stereoregular sequences is responsible for the occurrence of physical links. In this respect, copolymers should prove to be interesting experimental models to test the effects of length and content of regular sequences. Block copolymers made up of alternating crystallizable and uncrystallizable sequences can to some extent mimic these homopolymers that are anything but "stereocopolymers".

Curiously enough, until not long ago, systematic studies had only been performed on random copolymers.[12-14] Recently, we reported on an investigation[15] carried out with an organosilicic copolymer, poly(dimethylsiloxane)–poly[1-(dimethylsilyl)-4-(dimethylvinylsilyl)benzene], which was intended to throw some light on the gelation properties of this class of materials.

Here, we report on additional data that precisely deal with the effect of crystalline sequence composition. The thermodynamic properties through the temperature–concentration phase diagrams are established. These diagrams are of further use to account for the mechanical properties as a function of temperature and concentration and the swelling behavior.

Experimental Section

1. Synthesis. In this study a multiblock copolymer has been used, in which flexible poly(dimethylsiloxane) (PDMS) blocks and crystallizable "hard" blocks of poly[1-(dimethylsilyl)-4-(dimethylvinylsilyl)benzene] are associated. The crystalline block will be designated as COSP (crystalline organosilicic polymer) throughout this paper.

The synthesis of these block copolymers was first described by Prud'homme.[16] The method used is represented in Scheme I.

Further details concerning the preparation procedure can be found in ref 15 and 17.

Three samples with different contents of crystalline component (X_{COSP} in w/w) were synthesized. The experimental conditions were adjusted in order to obtain the following compositions: 10%, 20%, and 50%. The corresponding samples are designated as Copo10, Copo20, and Copo50, respectively.

Table I
Light-Scattering Characterization of Copo10 Carried Out at 60 °C

	solvent		
	chlorobenzene	toluene	decalin
	−0.1	−0.073	0.054
$M_{w\,app}$	220 000	215 000	225 000

2. Characterization. Light scattering from dilute solutions and gel permeation chromatography (GPC) were used to determine the different molecular weight averages.

Light-scattering measurements were carried out on a FICA 50 with a vertically polarized laser light of 546-nm wavelength. Refractive index increments were obtained by means of a Brice-Phoenix refractometer operating under the same conditions of temperature and wavelength.

Molecular weight characterization was carried out in different solvents at a temperature such that COSP crystallization was impeded (60 °C for Copo10 and Copo20 and 90 °C for Copo50).

The multiblock character was tested with Copo10 by using three solvents of differing refractive index following the method of Bushuk and Benoit.[18] No marked variation of the weight-average molecular weight was noticed (see Table I) which demonstrates this point.

Results are gathered in Table II. As can be seen from this table, Copo10 and Copo50 exhibit a weight-average molecular weight approximately twice larger as that of Copo20. Also worth mentioning is that the refractive index increments are in good agreement with those calculated from the theoretical copolymer compositions X_{COSP}.

GPC characterization was achieved at room temperature in toluene with a WISP 710B equipped with a refractometer from Shimazu. Accordingly, only the Copo10 and Copo20, which exhibit a very slow crystallization rate in toluene, were characterized by this technique. As usual, columns were calibrated with polystyrene standards of very narrow polydispersity. The results are given in Table II. While the calibration method is only strictly valid for homopolymers, the agreement is quite good with light-scattering data. The polydispersity of the samples corresponds to what is usually obtained for a polycondensation reaction.

3. Gel Formation. Gels were prepared from solutions in *trans*-decalin (99% trans). Homogeneous solutions were obtained by heating up to 175 °C appropriate blends of copolymer and solvent in a test tube. Then gelation was achieved through a rapid quench to −18 °C. For reasons given below, the gels were kept for a week at 30 °C prior to any measurements.

4. Techniques. Thermal Analysis. DSC II and DSC 4 from Perkin-Elmer were used. All the data were processed by means of the TADS system (thermal analysis data station). Experiments were performed at different heating rates. However, the standard

0024-9297/88/2221-1757$01.50/0

Scheme I

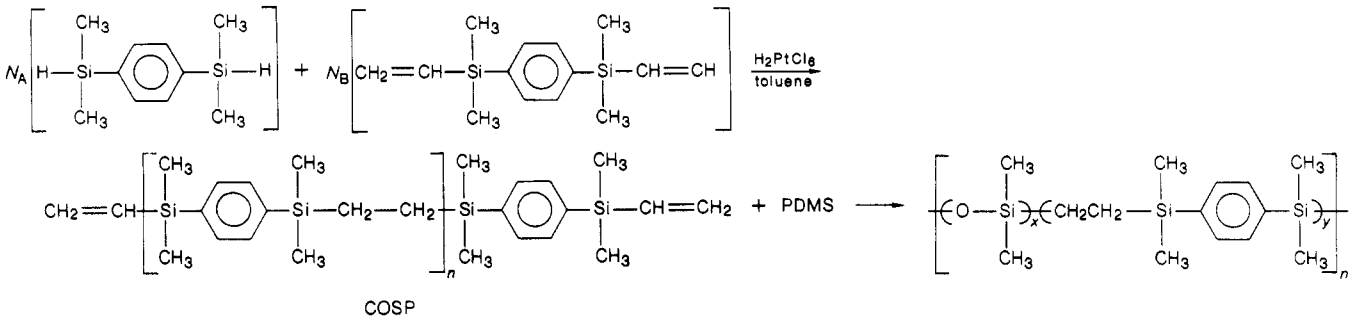

Table II
Characteristics of the Different Samples[a]

sample	$M_{n\,COSP}$	M_{nPDMS}	X_{COSP}	ν_{Copo}	$M_{w\,Copo}$ (2)	$M_{w\,Copo}$ (3)	$M_{n\,Copo}$ (3)	M_w/M_n
Copo10	2000	17 100	0.11	−0.073[b]	215 000	192 000	88 000	2.18
Copo20	4000	17 100	0.19	−0.06[b]	130 000	111 000	62 000	1.79
Copo50	9700	9700	0.5	−0.047[c]	290 000			

[a] 1 = theoretical, 2 = light scattering, 3 = GPC. [b] In toluene at 60 °C. [c] In tetralin at 90 °C.

20 °C/min heating rate was employed to establish the phase diagrams. Calibrations were achieved with an indium standard. To achieve solvent crystallization in the gel samples, low cooling rates were used (typically −2.5 to −1 °C/min).

Approximately 10 mg of freshly prepared gel was placed into a "volatile sample" pan which was then tightly sealed. In order to ensure a good gel-pan contact, the gel was remelted by heating the pan up to 175 °C; then the system was quenched again at −18 °C for 24 h. As stated above, the samples were finally kept at 30 °C for a week. While this last step does not markedly alter the overall thermal behavior, it allows one to appreciably improve the quality and resolution of the DSC thermograms.

Finally, in order to detect any solvent loss, the pans were systematically weighed after each experiment.

Turbidimetry. Turbidimetry experiments were carried out with a turbidimeter build by F. Debeauvais from our laboratory. A cooling rate of 10 °C/min was used.

X-ray Diffraction. X-ray characterization was carried out on a Sigma 2070 from CGR by means of a Debye-Scherrer camera (diameter 114.16 mm). A wavelength of $\lambda = 1.54$ Å produced from the Kα ray of copper was used.

Mechanical Properties. A mold with parallel surfaces was used so as to produce gel slabs of 1-cm thickness. These slabs were thermally treated as described above. Afterward, cylinders of 1.5-cm diameter were cut off to perform mechanical testing.

Compression moduli determination was carried out with a device described elsewhere.[19] The gels were kept immersed in water whose temperature was thermostatically controlled by an outer water circulation. Decalin and water are totally incompatible, which results in the absence of any alteration of the piece of gel. This procedure avoids the use of an excess of preparation solvent which would inevitably affect the gel swelling degree and correspondingly the gel mechanical response in time.

As usual, the compression modulus was determined from the relation

$$\sigma_R = E(\lambda - 1/\lambda^2)$$

where σ_R is the reduced stress and λ the strain ($\lambda = l/l_0$, l_0 being the initial sample height).

Results and Discussion

1. Thermal Behavior. Phase Diagrams. In a previous paper,[15] we showed that the system COSP–*trans*-decalin exhibits a miscibility gap, the existence of which is indirectly revealed by the crystal morphology and by a monotectic transition located near 50 °C. In the same paper is given the phase diagram for Copo20–*trans*-decalin gels which displays a monotectic transition. The occurrence of this transition led us to conclude that the gelation mechanism for samples quenched to well-below room temperature proceeds via liquid–liquid phase separation frozen in at its early stage by crystallization. Despite the fact that decalin is a good solvent for PDMS, this result therefore suggests that the solvent's quality toward the copolymer is mainly governed by the crystalline block.

Herein, additional results obtained on Copo10 and Copo50 gels confirm that a liquid–liquid phase separation does occur.

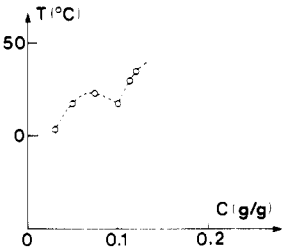

Figure 1. Turbidimetry experiments performed on cooling Copo50 solutions in *trans*-decalin at 10 °C/min.

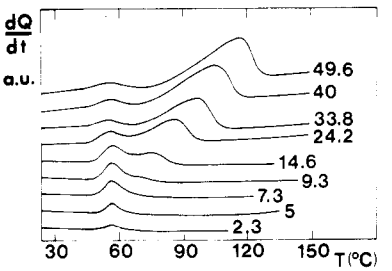

Figure 2. DSC thermograms from Copo50 gels quenched at −18 °C for 24 h then kept at 30 °C for a week. Heating rate 20 °C/min; concentrations as indicated (% w/w).

In Figure 1 are given turbidimetry measurements carried out on the Copo50–*trans*-decalin system as a function of copolymer concentration. This figure reveals quite distinctly the presence of a binodal.

Identical thermal behavior as that reported for Copo20[15] is also observed with Copo10 and Copo50. For instance, Figure 2 shows DSC traces for Copo50 gels at different copolymer concentrations. Temperature–concentration phase diagrams are given in Figure 3. For $C < C_M$, only one endotherm (the *low-melting endotherm*) is seen at $T_M \simeq 50$ °C. Conversely, for $C > C_M$, two endotherms are observed: again the low-melting endotherm whose temperature position is invariant with copolymer concentration and the *high-melting endotherm* the maximum of which

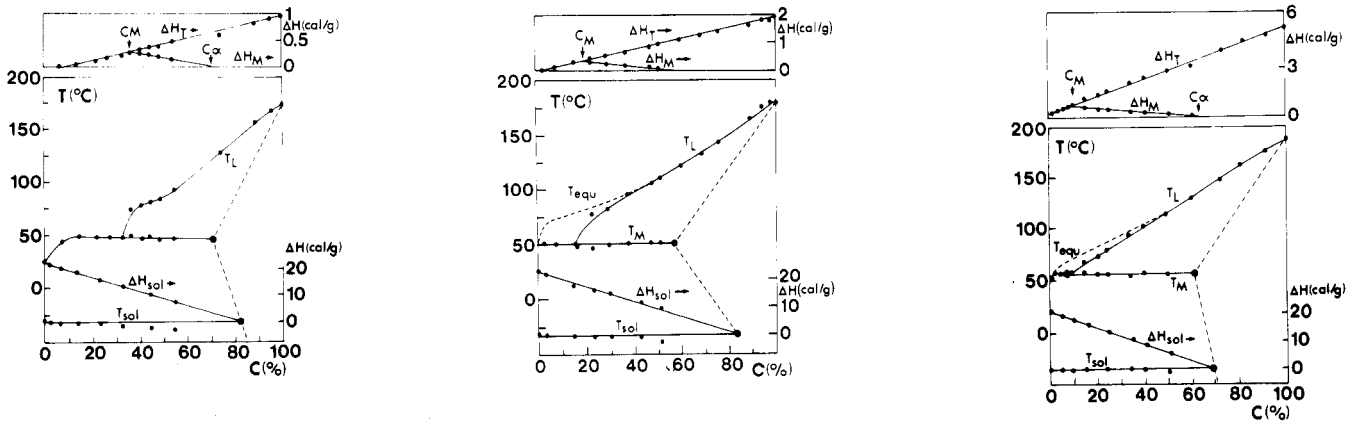

Figure 3. Temperature–concentration phases diagrams: (left) Copo10; (middle) Copo20 (from ref 15); (right) Copo50. Tamman's diagrams (ΔH versus C) are given on the same figures.

increases with increasing copolymer concentration. Also, the low-melting endotherm is much narrower than the high-melting endotherm. Whereas the high-melting endotherm area increases with increasing copolymer concentration, the low-melting endotherm eventually vanishes at the highest concentrations.

The low-melting endotherm accordingly reveals the occurrence of a monotectic transition near $T_M \simeq 50$ °C which arises from the effect on the gel melting properties of the liquid–liquid phase separation involved in the early stage of gel formation.[20] As can be noticed and as was abundantly commented on in ref 15, this monotectic transition is located well above the miscibility gap. This stems from the fact that, due to the possibility of reaching very high undercoolings, crystallization and fusion occur at temperatures well apart. The monotectic line simply represents a memory effect of the special conditions under which crystallization took place.

At higher concentrations, all the systems form a solid solution, which is characterized by a concentration C_α ranging between 0.6 and 0.7. Its structure is probably constituted of alternating domains made up of PDMS blocks swollen by solvent molecules on the one hand and COSP crystallites on the other hand.

The phase diagrams as well as the Tamman's diagrams (ΔH versus C) of Figure 3 reveal two differences depending upon copolymer composition:

(i) The monotectic transition temperature T_M slightly varies ($T_M \simeq 45$ °C for Copo10, $T_M \simeq 50$ °C for Copo20, and $T_M \simeq 55$ °C for Copo10). This is probably so because of the difference in COSP block length[17] ($M_{COSP} \simeq 9700$ for Copo50, $M_{COSP} \simeq 3900$ for Copo20, and $M_{COSP} \simeq 2100$ for Copo10). T_M simply reflects the difference existing between the melting points of the isolated sequences.

(ii) The concentration at the monotectic point C_M varies considerably ($C_M \simeq 9\%$ for Copo50, $C_M \simeq 18\%$ for Copo20, and $C_M \simeq 33\%$ for Copo10). The exact origin of this shift is currently unknown. It may stem from the fact that crystallization kinetics varies from one copolymer to another. As a matter of fact, the lower the content of crystalline component in the copolymer, the slower the crystallization kinetics. As a result, the concentration reached by the polymer-rich phase before crystallization, which is certainly related to C_M or even equal to it, should increase with decreasing the COSP amount in the copolymer.

Except for these differences, the phase diagrams are quite similar and show again that the gelation mechanism proceeds via liquid–liquid phase separation frozen in at its early stage by crystallization. This underlines that the quality of the solvent toward the copolymer is determined by the crystalline block even for a COSP content as low as $X_{COSP} = 10\%$.

Table III
Bragg Distances for COSP Samples (C = 100% and 50%) and Copo50 gel (C = 50%)[a]

d_{COSP}, Å	I	d_{Copo50}, Å	I
6.00	s	6.00	s
5.71	w	?	?
5.18	m	5.13	w
4.38	s	4.38	s
3.75	w	?	?

[a] I is the relative intensity; s = strong, m = medium, and w = weak. Other reflections can be seen with COSP samples but cannot be detected with Copo50 gel.

Finally, the thermal behavior and particularly the values of the total melting enthalpy (low- + high-melting endotherms) indicate that the gels owe their formation to crystallization of the COSP blocks with probably the same unit cell as in the bulk-crystallized COSP. This statement relies upon the extrapolation of the total melting enthalpy to $C = 1$, which gives, once normalized by the copolymer composition, a value close to what is found for pure crystallized COSP.[17]

This point has been further tested by X-ray diffraction experiments on the following samples: a bulk-crystallized COSP sample, a Copo50–*trans*-decalin sample ($C = 52\%$).

In Table III are reported the position and relative intensity of the different reflections. As can be seen, three reflections are still visible in the gel diffraction pattern which correspond both in position and intensity to those observed with the COSP homopolymer. Only the second reflection is no longer detectable in the case of the copolymer. Since this reflection is rather weak for the COSP sample, its absence in the gel sample diffraction pattern is not totally unexpected. Worth dwelling upon is that, unlike iPS (isotactic polystyrene) gels, no additional reflections are detected.[1]

2. Mechanical Testing. Stress relaxation and compression modulus have been investigated, the latter as a function of both temperature and concentration.

Stress Relaxation. In Figure 4 are drawn by means of a double-logarithmic scale the stress relaxation at constant deformation for different gels. As often observed, the relaxation is linear under this representation. Depending upon the system, the slope $m = \mathrm{d} \log \sigma / \mathrm{d} \log t$ varies between $m \simeq 0.01$ and 0.03. Such values are close to those found for chemically cross-linked gels,[21] that is, for systems with irreversible cross-links. Similar values are obtained with PVC gels for which there is strong evidence that gelation is due to crystallization of the syn-

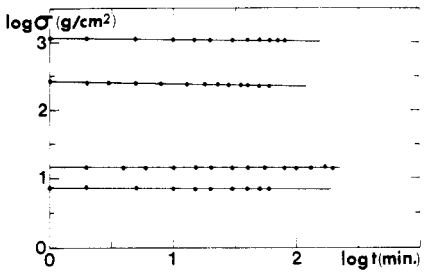

Figure 4. Stress relaxation, log σ_R (g/cm^2) versus log t (min), for $\lambda = 0.9$. From top to bottom: Copo50 for $C = 0.42$, $m = 0.023$; Copo50 for $C = 0.15$, $m = 0.03$; Copo10 for $C = 0.36$, $m = 0.01$; Copo20 for $C = 0.16$, $m = 0.03$.

diotactic sequences. Conversely, values reported for iPS gels contrast dramatically with those given here ($m_{iPS} \simeq$ 0.1–0.15). According to Guenet,[5] iPS gels do not owe their formation to a crystallization process. Rather, it is suggested that the structure is reminiscent of liquid crystals, a model which is consistent with the high mobility observed by stress relaxation.[10] If such an approach is correct, the value of m could be used as a criterion to differentiate crystalline from noncrystalline gels.

Compression Modulus. In a previous paper,[15] we developed a phenomenological theory intended to account for the variation of the compression modulus as a function of temperature. This theory is based on the concept of partial melting. It is considered that at T_M and for $C > C_M$ the gel partly melts, an approach contrasting with other views that regard the low-melting endotherm as the gel melting and the high-melting endotherm as the melting of chain-folded crystals. Whereas the latter approach pertains in the case of some physical gels, such as those prepared from iPS,[1] it does not hold in the present case. The partial melting concept is applied by assuming that, in a first approximation, the compression modulus is directly proportional to the content of polymer-rich phase. Since the polymer-rich phase is supposed to be the network itself, such an assumption seems then well-grounded. It ought to be, however, underlined that the mechanism involved at the molecular level remains to be elucidated. Considering the ratio $E(T)/E(20)$, where $E(T)$ and $E(20)$ are the moduli at T and 20 °C, respectively, one ends up with

for $C < C_M$

$$E(T)/E(20) = 1 \quad \text{for } T < T_M$$

$$E(T)/E(20) = 0 \quad \text{for } T > T_M$$

for $C > C_M$

$$E(T)/E(20) = 1 \quad \text{for } T < T_M$$

$$E(T)/E(20) = [(C_{prep} - C_{Ml}(T))/(C_{\alpha s}(T) - C_{Ml}(T))] \times (C_\alpha/C_{prep}) \quad \text{for } T > T_M \quad (1)$$

where C_{prep} is the preparation concentration and $C_{Ml}(T)$ and $C_{\alpha s}(T)$ are the concentrations defined by the liquidus and the solidus lines at T, respectively (note that at $T = T_M$, $C_\alpha = C_{\alpha s}(T)$ and $C_{Ml}(T) = C_M$).

In the same paper, it has been shown that the set of eq 1 can reproduce the experimental data gained on Copo20 gels provided that an appropriate solidus line be chosen. It must be stressed that there is practically no way of determining experimentally this line with accuracy, hence the use of two alternatives.

Here the same approach is used in an attempt to fit the experimental results gained on Copo10 and Copo50. As can be seen in Figure 5 the agreement is quite good with Copo10 gel samples. Conversely, there is an appreciable

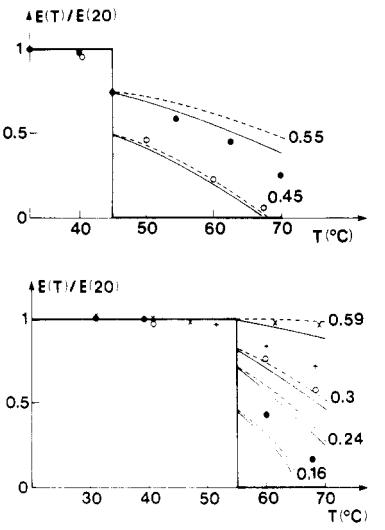

Figure 5. Variation of the compression modulus as a function of temperature. (a) Copo10 gels with $C_M = 0.33$, $T_M = 45$ °C, $C_\alpha = 0.7$; (○) $C = 0.45$, (●) $C = 0.55$. (b) Copo50 gels with $C_M = 0.09$, $T_M = 55$ °C, $C_\alpha = 0.61$; (●) $C = 0.16$, (○) $C = 0.24$, (+) $C = 0.3$, (×) $C = 0.59$. Theoretical variations calculated from relation 1: solid line = solidus constant with temperature in the range 20–70 °C; and dotted line = solidus varies as $aT + b$ (see ref 15).

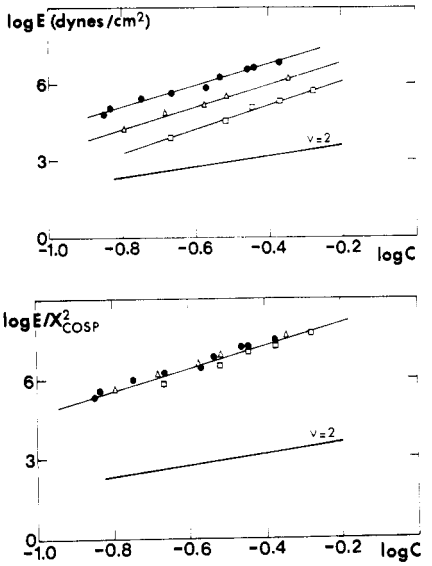

Figure 6. (a) Modulus versus concentration (log E versus log C): Copo50 (●); Copo20 (△); Copo10 (□). (b) log E/X_{COSP}^2 versus log C, symbols with the same meaning.

disagreement with Copo50 gel samples. The discrepancy is particularly marked for $C = 24\%$ and $C = 30\%$. A way of explaining this deviation consists of taking into account a possible recrystallization phenomenon. As a matter of fact, the phase diagram of Figure 3 represents the melting behavior for samples crystallized far from the equilibrium conditions. Under equilibrium conditions, the amount of liquid to solid phase would be lower. As a result, recrystallization can take place while the sample is kept in the measuring device for achieving temperature equilibration. Since crystallization kinetics of Copo50 is rather rapid for $T > T_M$, unlike that of Copo10 or Copo20, a recrystallization phenomenon is more liable to occur under these measuring conditions with this copolymer. This will eventually have some effect on the compression modulus.

The variation at constant temperature of the compression modulus as a function of copolymer concentration and composition has also been investigated. Figure 6a shows that the moduli vary as

$$E \sim C^{\omega} \quad (2)$$

where $\omega = 4.5 \pm 0.1$ independent of the copolymer sample. However, the magnitude of the modulus depends upon copolymer composition X_{COSP}. This variation is more explicitly written

$$E = (1.24 \pm 0.07) \times 10^9 \, X_{COSP}^2 C^{4.5\pm0.1} \ \text{dyn/cm}^2 \quad (3)$$

This is well illustrated by a universal plot log E/X_{COSP}^2 versus log C (Figure 6b).

Relation 3 emphasizes that copolymer concentration is, however, the determining factor. The exponent $\omega = 4.5 \pm 0.1$ is not predicted by any theories. Admittedly, theories developed for modulus versus concentration originally concern chemically cross-linked gels.[22] They do not take into account additional terms arising from the presence of crystals. The following and short analysis is an attempt to provide an explanation for this exponent.

The compression modulus is in principle related to the osmotic pressure Π exerted by a gel at swelling equilibrium conditions. Schematically speaking, it is related to the "need for dilution" of the system. In the case of chemical gels, where the only parameter is concentration, it has been shown in the frame of scaling laws that E and Π are directly proportional and read in good solvents[22] as

$$E \sim \Pi \sim C^{9/4} \quad (4)$$

In the case of physical gels, it is our feeling that two effects must be taken into account: (i) as with covalent gels, the effect of the osmotic pressure due to the network; (ii) the additional osmotic pressure arising from the presence of crystallites which will depend upon the degree of undercooling $\delta T = T_m - T_0$, that is the difference between the crystal melting temperature T_m (which increases with concentration) and the temperature, T_0, at which measurements are performed. Thus δT is a function of concentration.

For the sake of simplicity, we shall use a scaling argument and write E as

$$E \sim C^{\nu} F(\delta T) \quad (5)$$

where C^{ν} is the term which characterizes the network contribution and $F(\delta T)$ the undercooling effect. To conform to what is experimentally observed, one will approximate $F(\delta T)$ as

$$F(\delta T) \sim C^{\gamma} \quad (6)$$

so that E finally reads

$$E \sim C^{\nu+\gamma} \sim C^{\omega} \quad (7)$$

This type of argument suggests that the exponent for physical gels whose physical links are crystallites should be larger than what is found for covalent gels, especially when the undercooling degree displays marked variation with concentration. In this respect, worth mentioning are the results found by Walter on PVC gels.[23] This author reports exponents ranging from 3.12 up to 5.55 depending upon the solvent. Allegedly, the same type of argument as above should pertain for PVC since its propensity to form physical gels is due to its crystallization capacity.[24]

The exponent γ may be evaluated from the following argument. If one considers the systems at constant concentration, the modulus varies as X_{COSP}^2, that is, with a mean-field exponent. X_{COSP} is equivalent to a concentration. One may accordingly infer that this term is equivalent to the undercooling effect. Accordingly, the value of γ should be near $\gamma \simeq 2$. As a consequence, ν is estimated to $\nu \simeq 2.5$, a value which is now closer to what is obtained for covalent gels (2.25 in good solvents). It must be, however, stressed that such an exponent does not allow one to anticipate the gel structure (see ref 15).

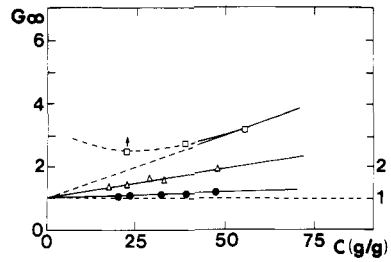

Figure 7. Equilibrium swelling degree G^{∞} as a function of preparation concentration C_{prep}: (□) Copo10; (△) Copo20; (●) Copo50.

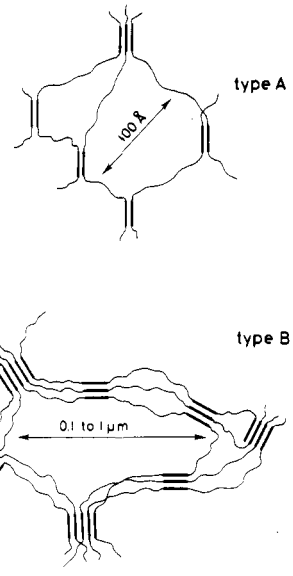

Figure 8. Two schematic types of fringed micelle models: type A is characterized by a short mesh and is close to the structure encountered in covalent gels; type B is characterized by a larger mesh and by fiberlike entities. This morphology is frequently observed in physical gels.

3. Swelling Behavior. Due to the very chemical structure of the copolymer, swelling is expected once a piece of gel is immersed in an excess of *trans*-decalin. One way of evaluating the swelling degree G consists of taking the ratio

$$G = P/P_0 \quad (8)$$

where P_0 is the sample's weight prior to immersion and P is that after immersion for a given time. The equilibrium swelling ratio G^{∞} is then defined for infinite time, but in practice, 1 month is quite enough.[15] Experimental results are drawn in Figure 7 for the three copolymer samples.

In a previous publication,[15] we examined the swelling behavior of Copo20 gels in the light of the two molecular models portrayed in Figure 8. The fringed micelle of type A is reminiscent of what is encountered in covalent gels. Numerous theories are available for the latter type of gel and particularly scaling approaches are well-suited to describe them.[22] The "C^* theorem" proposed by de Gennes[22] states that the gels should swell up to the overlap concentration C^* of the chains joining the covalent knots. C^* is given by

$$C^* = 3M/4\pi R^3 N_A \quad (9)$$

where R is the radius of gyration of a "unit" chain, M its molecular weight, and N_A Avogadro's number.

G^{∞} should then be

$$G^{\infty} = C_{prep}/C^* \quad (10)$$

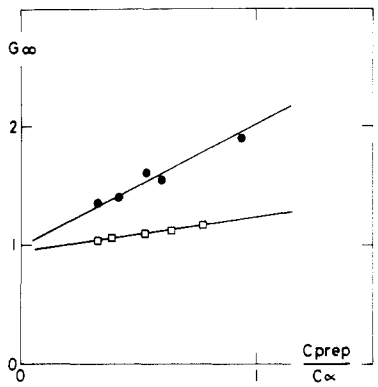

Figure 9. Equilibrium swelling degree G^∞ as a function of C_{prep}/C_α: (●) Copo20; (□) Copo50.

Network defects such as trapped entanglements are not taken into consideration by this approach. Yet, it has been shown to hold in a wide range of concentration.[25]

If a possible size effect of the crystallites is ignored, this approach can be applied to the type A model. Estimating C^* for $M_{POMS} = 9700$ through the experimental relation $R = 0.14M^{0.6}$,[26] a slope of 0.08 instead of unity is found for the variation of G^∞ as a function of C_{prep}/C^* in the case of Copo50 gels. In our opinion such a discrepancy is too large to be attributed to defects. We therefore come to the same conclusion we drew with Copo20 gels, (the case of Copo10 will be discussed later on).

Another model, designated as a fringed-micelle model of type B (see Figure 8), can be tested. It ought to be mentioned that such a model, whose features are fiberlike, is derived from optical and electron microscopy observations made on various physical gels.[4,27,28]

He et al. have derived[15] the equilibrium swelling degree for this model by assuming that only the polymer-rich phase is liable to swell up to a concentration C_γ. From simple arguments, G^∞ reads as

$$G^\infty = 1 + (C_\alpha/C_\gamma - 1)(C_{prep}/C_\alpha) \qquad (11)$$

In Figure 9 are replotted the data for Copo50 and Copo20 as a function of C_{prep}/C_α. From the slope, one obtains $C_\gamma \simeq 0.51$ for Copo50 and $C_\gamma \simeq 0.27$ for Copo20. While such values seem realistic, the determination by another technique of the local concentration in the amorphous domain, that is, C_γ, is much needed to further test this approach.

The case of Copo10 gels is somewhat at variance with the two other. First, a 22.5% gel does not reach equilibrium even after a month. Second, there is significant deviation from linearity. We attribute these effects to the disruption of some crystalline domains. The swelling of the amorphous domains of the polymer-rich phase, which probably induces shear stress, is capable of causing the disappearance of the less stable crystals. Neither the analysis based on the analogy with covalent gels nor the approach derived from the model of type B can describe this behavior. A deeper knowledge of the molecular structure after swelling is needed here.

Concluding Remarks

As outlined in the Introduction, the knowledge of physical gelation of multiblock copolymers may prove useful for understanding that of atactic homopolymers.

In this respect, it is our feeling that the case of poly(vinyl chloride), PVC, deserves special discussion in the light of the present results. As a matter of fact, atactic PVC can show a crystallinity of about 10% in the bulk state which is due to the crystallization of the syndiotactic sequences.[29,30] Gelation has also been attributed to a crystallization phenomenon involving the same sequences.[30-32] Therefore, Copo10 and PVC gels should be directly comparable. Yet, a comparison between compression modulus values reveals a huge discrepancy. For example, the compression modulus of a 28% PVC gel in bromonaphthalene[33] is $E_{PVC} \simeq 4 \times 10^6$ dyn/cm^2, whereas we found $E_{Copo10} \simeq 4 \times 10^4$ dyn/cm^2 for Copo10 gels at the same concentration. There are 2 orders of magnitude which cannot be only accounted for by the unlikeliness of the chemical nature. Admittedly, the amount of physical links is underestimated in PVC gels. These remarks meet recent conclusions by Mutin et al.,[34] who claim, on the basis of light-scattering studies on PVC aggregates, that two types of links exist. One type is said, as usual, to arise from crystallization of the highly syndiotactic sequences, whereas the other type is supposed to be due to associations of less regular sequences.[30,34]

Acknowledgment. X. He is indebted to the government of the People's Republic of China for a grant in aid.

References and Notes

(1) Girolamo, M.; Keller, A.; Miyasaka, K.; Overbergh, N. *J. Polym. Sci., Polym. Phys. Ed.* **1976**, *14*, 39.
(2) Wellinghoff, S. J.; Shaw, J.; Baer, E. *Macromolecules* **1979**, *12*, 932.
(3) Sundararajan, P. R.; Tyrer, N. J.; Bluhm, T. L. *Macromolecules* **1982**, *15*, 286.
(4) Guenet, J. M.; Lotz, B.; Wittmann, J. C. *Macromolecules* **1985**, *18*, 420.
(5) Guenet, J. M. *Macromolecules* **1986**, *19*, 1960.
(6) Tan, H. M.; Hiltner, A.; Moet, H.; Baer, E. *Macromolecules* **1983**, *16*, 28.
(7) Gan, Y. S.; François, J.; Guenet, J. M. *Macromolecules* **1986**, *19*, 173.
(8) Delmas, G.; Et al. *Macromolecules* **1984**, *17*, 1200; **1985**, *18*, 1235.
(9) Smith, P.; Lemstra, P. J. *J. Mater. Sci.* **1980**, *15*, 505.
(10) Guenet, J. M.; McKenna, G. B. *J. Polym. Sci., Polym. Phys. Ed.* **1986**, *24*, 2499.
(11) Jelich, L. M.; Nunes, S. P.; Paul, E.; Wolf, B. A. *Macromolecules* **1987**, *20*, 1943.
(12) Berghmans, H.; Govaerts, F.; Overbergh, N. *J. Polym. Sci., Polym. Phys. Ed.* **1979**, *17*, 1251.
(13) Takahashi, A. *Polymer J. (Tokyo)* **1973**, *4*, 379.
(14) Domszy, R. C.; Alamo, R.; Edwards, C. O.; Mandelkern, L. *Macromolecules* **1986**, *19*, 310.
(15) He, X.; Herz, J.; Guenet, J. M. *Macromolecules* **1987**, *20*, 2003.
(16) Prud'homme, C. Thesis, University of Strasbourg, 1980.
(17) He, X. W.; Fillon, B.; Herz, J.; Guenet, J. M. *Polym. Bull. (Berlin)* **1987**, *17*, 45.
(18) Benoit, H.; Bushuk, A. *Can. J. Chem.* **1958**, *36*, 199.
(19) Belkebir-Mrani, A.; Herz, J.; Rempp, P. *Makromol. Chem.* **1977**, *178*, 485.
(20) One may wonder whether this transition at 50 °C or so does not arise from the melting of crystals formed during the gelation process and then thickened by annealing at 30 °C (this question was raised by reviewer I). Two arguments allow dismissal of such a hypothesis: (i) There is no reason to believe that the thickening would occur in such a way as to make the crystal melting point invariant with temperature. (ii) Thickening cannot explain why the ΔH of this transition goes through a maximum and then decreases at higher concentrations. This process should be uniform, independent of polymer concentration.
(21) Thirion, P.; Chasset, R. *Chim. Ind., Genie Chim.* **1967**, *97*, 617.
(22) de Gennes, P. G. *Scaling Concepts in Polymer Physics*; Cornell University: Ithaca, NY, 1979.
(23) Walter, A. T. *J. Polym. Sci.* **1954**, *23*, 207.
(24) Dorrestijn, A.; Keijzers, A. E.; te Nijenhuis, K. *Polymer* **1981**, *22*, 305.
(25) Munch, J. P.; Candau, S. J.; Hild, G.; Herz, J. *J. Physiol. (Paris)* **1977**, *58*, 971.
(26) Beltzung, M.; Herz, J.; Picot, C. *Macromolecules* **1983**, *16*, 580.
(27) Stamhuis, J. E.; Pennings, A. J. *Br. Polym. J.* **1978**, *10*, 221.
(28) Toyama, K.; Miller, W. G. *Nature (London)* **1981**, *289*, 813.
(29) Lemstra, P. J.; Keller, A.; Cudby, M. *J. Polym. Sci., Polym. Phys. Ed.* **1978**, *16*, 1507.
(30) Juijn, J. A.; Gisolf, A.; de Jong, W. A. *Kolloid Z. Z. Polym.* **1973**, *251*, 456.

(31) Takahashi, A.; Nakamura, T.; Kagawa, I. *Polym. J. (Tokyo)* **1972**, *3*, 207.
(32) Haas, H. C.; McDonald, R. L. *J. Polym. Sci., Polym. Phys. Ed.* **1973**, *11*, 1133.
(33) Mutin, P. H. Thesis, University of Strasbourg, 1986. Mutin, P. H.; Guenet, J. M., submitted to *Macromolecules*.
(34) Mutin, P. H.; Guenet, J. M.; Hirsch, E.; Candau, S. J. *Polymer* **1988**, *29*, 30.

Deformation-Dependent Properties of Polymer Networks Constructed by Addition of Cross-Links under Strain

L. G. Baxandall* and S. F. Edwards

Cavendish Laboratory, Madingley Road, Cambridge CB3 OHE, U.K. *Received July 17, 1987; Revised Manuscript Received October 13, 1987*

ABSTRACT: Final network properties (elasticity and structure factor) are calculated for polymer networks which are constructed by addition of cross-links at a series of deformations. It is shown that the m-network hypothesis (the generalization of the two-network hypothesis first proffered by Andrews, Tobolsky, and Hanson) is valid as an interpretation of the free energy of deformation. A simple modification of this hypothesis allows for a similar interpretation of the structure factor.

Introduction

Both the microscopic and macroscopic (bulk) properties of a polymer network are influenced by the construction history of the network. As a corollary to this a complete knowledge of the cross-linking history of a network is required for any prediction of the final network properties.

A specific case in which this complete knowledge is in principle available is that of a network produced from a basis network, whose structure is known, through a well-defined sequence of addition of cross-links at different strains of this basis network. The history of the network is then characterized by the sequence of these strains and the number of cross-links introduced at each strain. A network constructed in this way for which crosslinks once introduced are always stable (not liable to subsequent breakage) we shall term an addition network.

Experimentally such networks can be constructed through irradiation of basis networks held at a series of deformations, the irradiation acting as a cross-linking agent.

This paper will present a calculation of certain final network properties—the macroscopic elasticity and the microscopic structure factor—of such addition networks for a general history of cross-linking. The results of this calculation for the free energy of deformation $F(\lambda)$ of the final addition network and the structure factor $S(k,L,\lambda)$ for the same are

$$F(\lambda) = \tfrac{1}{2}k_B T \sum_{i=0}^{M} N_i \,\mathrm{Tr}\,(\lambda^T(\lambda_i^T\lambda_i)^{-1}\lambda)$$

and

$$S(k,L,\lambda,p,p') = \exp\Bigg[-k^2 f(\Omega_M,p,p') + \Bigg[\frac{l^2}{6}|p-p'| - f(\Omega_0,p,p')\Bigg]\mathrm{Tr}\,(\mathbf{k}\lambda^T\lambda\mathbf{k}) + \sum_{i=1}^{M}\mathrm{Tr}\,(\mathbf{k}\lambda^T(\lambda_i^T\lambda_i)^{-1}\lambda\mathbf{k})[f(\Omega_{i-1},p,p') - f(\Omega_i,p,p')]\Bigg]$$

where

$$S(k,L,\lambda) = (1/L^2)\int_0^L dp \int_0^L dp'\, S(k,L,\lambda,p,p')$$

λ here denotes the final deformation matrix of a network which is constructed by addition of N_i cross-links at a series of deformations λ_i. The number of such intermediary deformations is M, and the basis network (deformation "1") is constructed by addition of N_0 cross-links to an uncross-linked melt. L is the length of labeled chain, which produces the scattering at wave vector $\mathbf{k}$ while Ω_i is equal to $(6/L_{tot})(N_0 + \ldots + N_i)$ and $f(\Omega_i,p,p')$ is $(1/2\Omega_i)(1 - \exp(-\frac{1}{6}l\Omega_i|p-p'|))$. k_B is Boltzmann's constant, T the absolute temperature, and L_{tot} the total length of chain within the network.

We will also give an interpretation of these results in the light of the independent network hypothesis first proffered by Andrews, Tobolsky, and Hanson.[1]

Formulation of the Problem

The basis of the calculation is the evaluation of the partition function for an amorphous rubber as first performed by Edwards[2] and furthered subsequently by Fricker.[3]

1. The Description of a Network. A network is taken to be fully characterized by its connectivity. This connectivity has two facets. First, the connectivity associated with the initial uncross-linked chains (the linkage of successive monomers to form a polymer) and, second, that due to added cross-links. For a high degree of cross-linking the effect of free ends is minimal and the initial uncross-linked connectivity can be summarized as a single polymer of arc length the same as the total arc length of many polymers. The effect of this is to explicitly eliminate free ends. One can then assign to each monomer segment in the system an arc position along this single chain. The subsequent cross-link constraints are then summarized by specifying the arc coordinates which are tied by each cross-link.

In the calculation, the connectivity of the uncross-linked chain is represented by the conventional Wiener measure form (the continuous limit of a chain of discrete links),

$$P\{R(s)\} = \exp\left(-\frac{3}{2l}\int_0^{L_{tot}} R'^2\, ds\right) \qquad (1)$$

where $\{R(s)\}$ is a configuration of the polymer in which the spatial position R of each arc point s is specified, l is the Kuhn length, and L_{tot} is the total length of polymer, R' denotes $\partial R/\partial s$.

0024-9297/88/2221-1763$01.50/0